Detection of Turbulent Boundary-Layer Separation Using Fluctuating Wall Pressure Signals

Richard A. Gramann* and David S. Dolling†
The University of Texas at Austin, Austin, Texas

A technique for detecting intermittent, shock-induced, turbulent, boundary-layer separation has been developed and tested in a Mach 5 blowdown tunnel. The interactions were generated by "semi-infinite" circular cylinders. The method employs two miniature pressure transducers oriented streamwise and installed flush with the test surface. Through cross correlations of the conditionally sampled signals of the two transducers under the moving shock, it has been shown that the flow downstream of the instantaneous shock position is separated. The results indicate that in these flows, the separation location obtained from surface tracers, such as the kerosene lampblack method, is actually the downstream boundary of a region of intermittent separation.

Introduction

SURFACE tracer techniques, such as the kerosene lampblack method, are widely used in high-speed flows to find "separation lines" or "lines of coalescence" particularly in shock-wave turbulent boundary-layer interactions.[1] These methods are relatively easy to use and produce highly defined, repeatable "separation lines." In the case of the kerosene lampblack method, in which the pattern is lifted off the surface on large sheets of transparent tape, full-scale undistorted records are obtained. Measurements of angles and length scales are easily made from these patterns and are widely used for comparison with numerical simulation results.

In many shock-wave boundary-layer interactions, wall pressure fluctuation measurements have shown that the separation shock is unsteady generating an intermittent wall pressure signal.[2-7] A typical example, in a Mach 3 blunt fin interaction, is shown in Fig. 1. This region of shock motion is known as the intermittent region. Intermittency γ is defined as the fraction of time a pressure transducer is downstream of the shock and is an indication of location within the intermittent region. The intermittent region extends from where the incoming flow is first disturbed, to close to the separation line S, indicated by surface tracers.

In such flows where the separation shock is highly unsteady, the physical meaning of these surface tracer lines comes into question. In particular, does backflow actually occur upstream of the surface tracer line? This might occur since the surface tracer material responds to the mean-wall shear stress, and the technique has essentially zero frequency response. Further, the mean-wall shear stress at a point in the intermittent region is the result of two flowfields (i.e., the undisturbed flow upstream of the shock and the "disturbed" flow downstream of the shock). What is needed to understand what the surface tracer lines in this region actually represent are instantaneous flow direction measurements close to the surface. Unlike incompressible flow, for which instantaneous flow direction measurement techniques such as thermal tufts are reasonably well developed,[8,9] no relatively straightforward measurement techniques have been developed for high-speed flows. Therefore, the need for a relatively simple method of detecting "instantaneous" flow direction is clearly evident.

Received Sept. 30, 1988; revision received July 5, 1989.

*Graduate Research Assistant. Member AIAA.
ing and Engineering Mechanics. Member AIAA.
†Associate Professor, Department of Aerospace Engineering and Engineering Mechanics. Associate Fellow AIAA.

The objective of the work reported in this paper was to determine if flow direction could be deduced from wall pressure fluctuations. A method of doing this, using high-frequency response pressure transducers, has been developed and tested in a Mach 5 shock-wave turbulent boundary-layer interaction. Although considerable care is needed in transducer installation, calibration, and use, such measurements are nonintrusive and can be made relatively easily and routinely in high-speed flows. The equipment, technique, analysis involved, and some results are presented in this paper.

Experimental Program

Wind Tunnel and Test Conditions

All data were obtained on the tunnel floor of the University of Texas Blowdown Wind Tunnel under essentially adiabatic wall temperature conditions. The facility has a 17×15 cm test section and operates at a nominal freestream Mach number of 4.9. The boundary layer developed naturally and was fully turbulent at the test location. Table 1 gives the incoming boundary layer and freestream properties as deduced from pitot

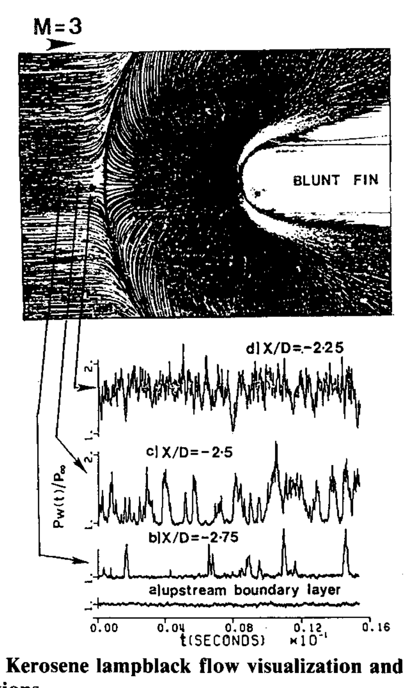

Fig. 1 Kerosene lampblack flow visualization and wall-pressure fluctuations.

Table 1 Freestream and boundary-layer conditions

Parameter	Tunnel floor
	Wind tunnel flow conditions
M_∞	$4.90 \pm .02$
U_∞	741 m/s (2432 ft/s)
Re_∞	53.3×10^6 m^{-1} (16.2×10^6 ft^{-1})
T_0	330 K (595 R)
P_0	2.09×10^6 N/m^2 (304 psi)
X	0.74 m (29 in.) from throat
δ_0	1.62×10^{-2} m (0.63 in.)
δ^*	5.23×10^{-3} m (0.206 in.)
θ	4.54×10^{-4} m (1.83×10^{-2} in.)
Π	0.115
Re_θ	23.4×10^3
C_f	9.9×10^{-4}

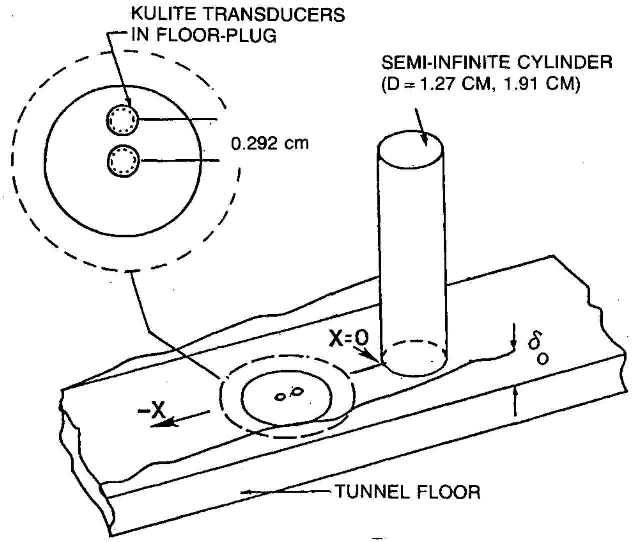

Fig. 2 Model and coordinate system.

surveys. Standard terminology is used. The models used for the study were circular cylinders, 1.27 and 1.9 cm in diameter, 8.9 cm and 7.6 cm high, respectively. Based on the criterion of Ref. 10, both cylinders were effectively semi-infinite. The position of the cylinders could be varied relative to the fixed location of the instrumentation plug described below so that different regions of the flowfield could be examined (see Fig. 2).

Instrumentation

A circular instrumentation plug was installed flush with the tunnel floor approximately 0.74 m from the nozzle throat. The cylinders were mounted a short distance downstream of the instrumentation plug location. Wall pressure measurements were made using miniature high-frequency pressure transducers. Kulite XCQ-062-15A or XCQ-062-50A transducers were used for all tests. These transducers have a full-scale range of 15 psia and 50 psia with nominal sensitivities of 13 mV/psi and 2 mV/psi, respectively. Both have a pressure-sensitive diaphragm 0.071 cm (0.062 in.) in diameter with a fully active Wheatstone bridge atomically bonded to it. The estimated frequency response of the transducers, when equipped with perforated screens to protect the silicon diaphragm, is approximately 50 kHz. Calibration of the transducers was performed statically. Earlier work[11] has shown that static calibrations are within a few percent of dynamic calibrations. In all cases, the transducers were mounted flush with the plug surface with a streamwise spacing of 0.292 cm center to center.

Signals from the pressure transducers were amplified with a gain of 200–500 and analog filtered at 50 kHz. The signals were digitized by a 12-bit A/D converter (0–10 V input) at

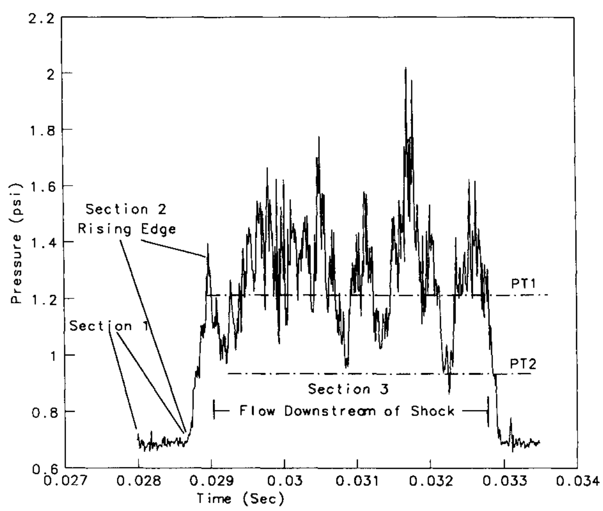

Fig. 3 Upstream transducer pressure time signal components.

sampling rates of 200, 250, 333, and 500 kHz per channel and stored on magnetic tape. In each test, 70-400 records per channel of data (1 record = 1024 data points) were taken. All data acquisition and subsequent analysis were performed on a MASSCOMP MC-5500 series minicomputer.

Cross Correlation Analysis Method

The purpose of this analysis was to determine if the flow direction immediately downstream of the separation shock could be deduced from wall pressure fluctuations. Since the direction of the undisturbed boundary layer flow upstream of the shock is known, the moving shock wave is the instantaneous upstream boundary of a flowfield, whose flow direction near the wall must be determined. Only those data corresponding to flow downstream of the shock were needed in order to analyze the flow in this region. Therefore, the first step was the development of an algorithm to isolate that fraction of the pressure signal corresponding to flow downstream of the shock. Two methods were devised and tested—both yielded similar results.

In both techniques, a two-threshold method was used. In all cases, the upstream transducer signal was used to determine when both transducers were downstream of the shock. If the upstream transducer is downstream of the shock, it follows that the downstream transducer must be also. Examining the pressure signal from the upstream transducer (see Fig. 3), there are three principle components. The first component, section 1, corresponds to undisturbed boundary-layer flow upstream of the separation shock. Section 2, the second component, is the pressure rise (or fall) due to the shock passing over the transducer. Section 3 corresponds to fluctuations downstream of the shock. These fluctuations have a minimum pressure. Pressure fluctuations downstream of the shock rarely drop below this minimum pressure. This pressure was estimated by visual inspection of the signal and the second threshold (PT2) was set to this minimum pressure.

The first threshold (PT1) was set by visual inspection also. PT1 was set at a value approximately equal to the mean of the pressure fluctuations downstream of the shock. This pressure is large enough to eliminate most of the rising edge due to the shock passage (section 2) from being classified as flow downstream of the shock. Once the pressure exceeds PT1, it corresponds to flow downstream of the shock until the pressure falls below PT2. Once the pressure falls below PT2, the pressure must then exceed PT1 to indicate a new section of data corresponding to flow downstream of the shock.

These thresholds (PT1 and PT2) were constant for an entire data file. Figure 4 shows a typical time history on both channels. Several shock passages can be seen. Since each passage is different, the thresholds are not ideal for every passage. This results in valid data being discarded, or shock passage (rising edge) data may be included as data corresponding to flow downstream of the shock. A sensitivity study was performed to investigate the influence of the threshold settings on the results. The results are not particularly sensitive to physically reasonable settings. A brief discussion of this study is presented in the Appendix.

In addition to the two-threshold method (TTM), another method was developed. This method worked exactly as the TTM, except a further constraint was added. Once the pressure exceeded PT1, the maximum point on the rising edge was found. This point was used as the section 2/section 3 boundary. Section 3 began after this point. This algorithm is known as the "top-finding" algorithm. Its purpose was to help eliminate some of the errors due to two constant thresholds. There was no significant difference in the results between the two methods. A further discussion of the method sensitivities is included in the Appendix.

The technique for finding flow direction relies on the cross correlation of two fluctuating pressure signals from two streamwise transducers located relatively close to each other. The cross-correlation equation is

$$R_{pp}(\tau) = \Sigma p_1(t) \times p_2(t+\tau)$$

where $p_1(t)$ is the upstream channel of pressure data, $p_2(t)$ is the downstream channel of pressure data, and τ is the time delay between channels.

In general, for continuously sampled data, cross correlations are not calculated as shown but are computed using Fast Fourier Transform (FFT) algorithms. FFT methods were developed to reduce the computation time needed for the analysis of large data sets. Typically 512- or 1024-point transforms are calculated, and the correlation coefficients are averaged over many records. The time savings in using an FFT algorithm on a small data sample is not nearly as great. Also, the algebraic calculation is much simpler to code especially when the calculation data set size needs to be flexible as was the case here, as described below. Thus the cross correlations in this analysis were calculated algebraically.

The mechanics of the calculation of cross correlations downstream of the shock proceeded as follows. The number of data points (NI) desired for each "conditionally extracted analysis data set" (CEADS), typically 32, 64, or 128 points is input to the code. One such data set, bracketed by the hatched lines, is shown in Fig. 4. The number of points chosen depends on the intermittency of the data. Data at high intermittencies have longer continuous blocks of data behind the shock and thus allow longer CEADS. Low intermittency values require shorter CEADS. The data file was systematically searched for blocks of data, NI points in length, that corresponded to flow downstream of the shock (section 3, Fig. 3). Each time a block was found, it formed a CEADS. This data set was algebraically cross correlated with the corresponding data points from the downstream transducer. Once the cross-correlation calculations were complete, the coefficients were normalized by the product of the root mean square of the CEADS for each channel in the data set and added to a cumulative results array. Then the next block of NI points corresponding to flow downstream of the shock was found and the process repeated. When all data were analyzed, the results array was normalized by the number of CEADS analyzed.

Discussion of Results

For reference purposes when discussing the cross correlations from the conditional analysis algorithm in the intermittent region, Fig. 5 shows a standard 1024-point FFT cross-correlation result from 400 records of data taken with two pressure transducers located in the undisturbed turbulent boundary layer. The single maximum at positive τ_0 is generated by turbulent eddies traveling downstream. From τ_0 and the transducer spacing, the broadband convection velocity of the pressure carrying eddies can be calculated. Its value of 0.67 U_∞ (496 m/s), obtained by interpolation of the data points bracketing the maximum, agrees reasonably well with previous work.[12] In contrast, downstream of S, the separation line from the surface tracer experiments, two maxima in R_{pp} are evident and correspond to two physical phenomena (see Fig. 6). The $R_{pp\max}$ at positive time delay corresponds to pressure fluctuations due to eddies in the separated shear layer flowing downstream. The broadband time delay for maximum correlation of these structures is $\tau = 0.006$–0.008 ms giving a downstream convection velocity in the range 365–487 m/s. This velocity is less than that in the undisturbed boundary layer since the flow has gone through the separation shock wave. The second phenomenon is back flow in the recirculating/vortical separated region. This back flow generates the peak at $\tau = -0.016$ to -0.018 ms corresponding to a broadband upstream velocity of 162–183 m/s.

As discussed earlier, the conditional analysis cross-correlation code was written to analyze signals in the intermittent region. Figure 7 shows correlations at five stations in the intermittent region for the 1.9-cm diameter cylinder. The legend indicates the normalized streamwise station of each transducer, the intermittency of the upstream channel, and the

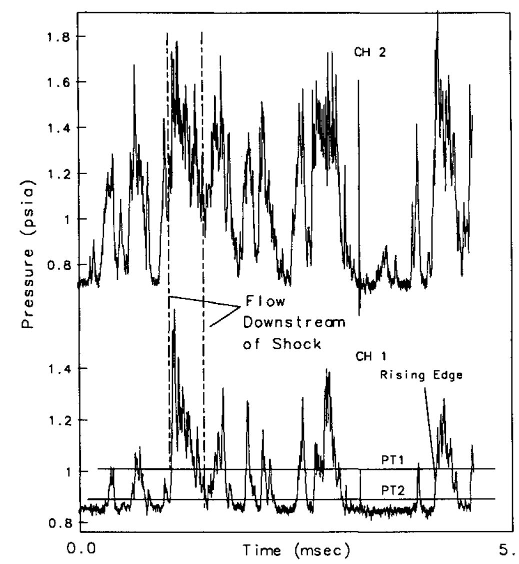

Fig. 4 Pressure time histories and conditional algorithm thresholds.

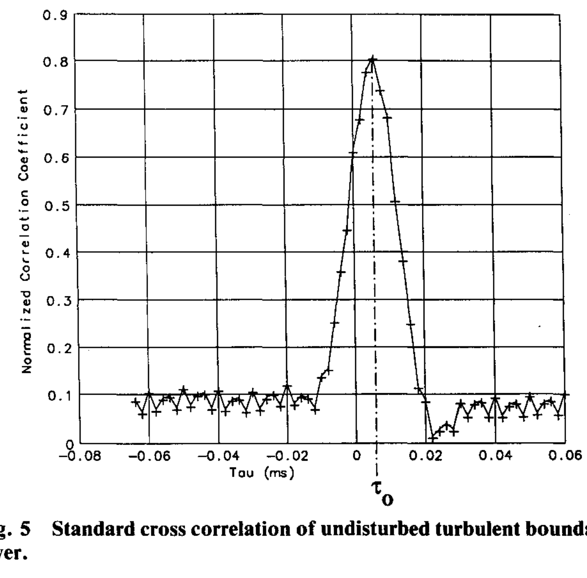

Fig. 5 Standard cross correlation of undisturbed turbulent boundary layer.

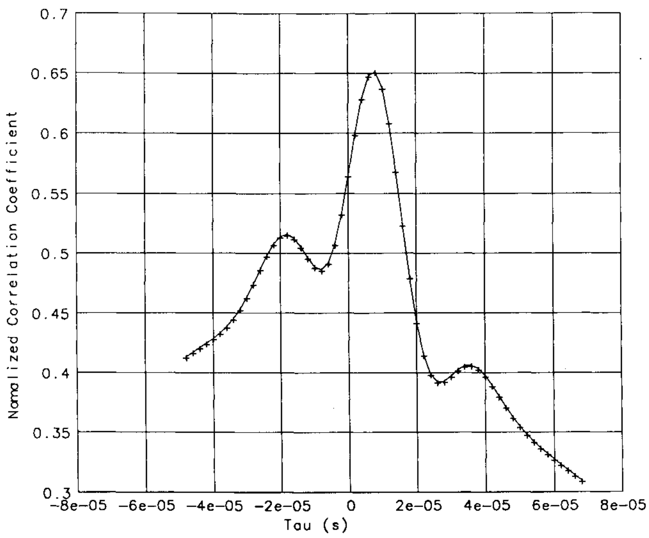

Fig. 6 Standard cross correlation of flow downstream of *S*.

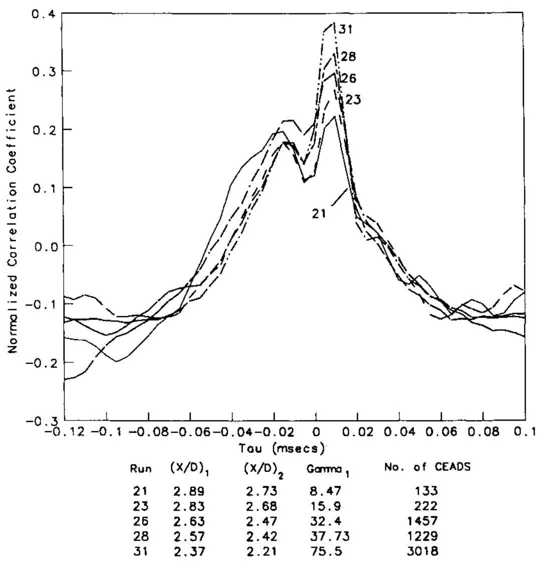

Fig. 7 Cross correlations of CEADS, 1.9 cm cylinder.

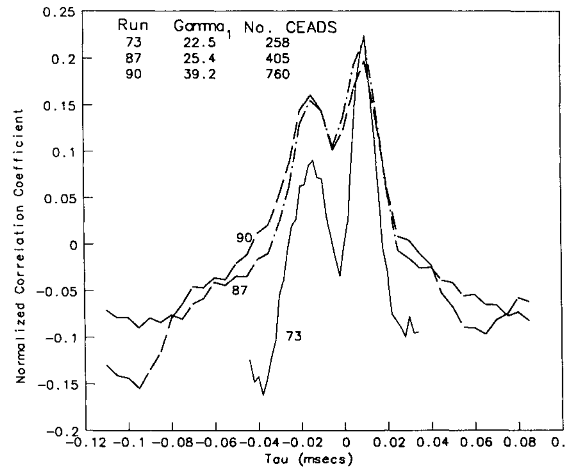

Fig. 8 Cross correlations of CEADS, 1.27 cm cylinder.

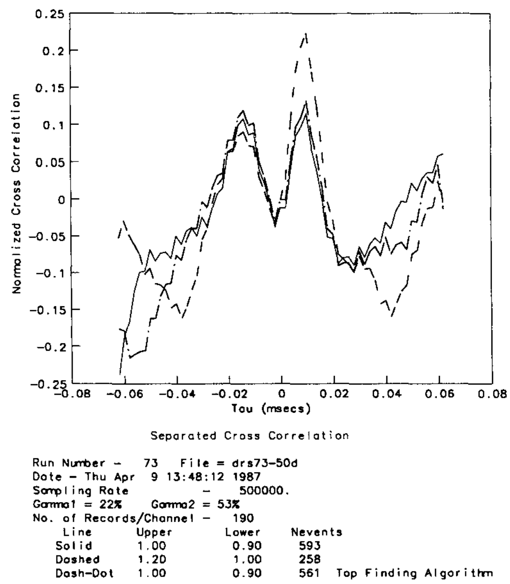

Fig. 9 Sensitivity of cross correlation of CEADS.

number of CEADS used to calculate each curve. At all values of intermittency, the "double peak" characteristic of separated flow can be seen. The positive and negative values of τ at which these maxima in R_{pp} occur are the same in all five cases. Based on the transducer spacing and τ, the broadband upstream and downstream velocities are in the ranges of 195-292 and 292-584 m/s, respectively. The boundaries of these ranges are calculated using the data points bracketing the peaks. From linear interpolation the actual maxima are about midway between these points giving upstream and downstream velocities of 234 and 390 m/s, respectively. Taking into account the lower sampling rates for the data sets in the intermittent region and the reduced time resolution of the cross correlations, these velocities are essentially the same as those calculated from Fig. 6. These results show clearly the flow structure downstream of the instantaneous shock location is the same at all stations within the intermittent region. Further, it is the same as the flow structure in the separated flow downstream of *S*.

Figure 8 shows cross correlations using the 1.27-cm diameter cylinder. All three stations show the characteristic double peak indicating back flow immediately behind the shock. No variation in time delay at $R_{pp\max}$ is seen. $R_{pp\max}$ occurs at $\tau = -0.014$ ms and $\tau = 0.08$-0.01 ms giving upstream and downstream velocities of about 209 and 292-365 ms, respectively. Examination of Figs. 7 and 8 reveals that both cylinders have the same time delays for both peaks, within the sampling rate accuracy, indicative of the same flow structure immediately downstream of the shock.

All results discussed up to this point have been the averaged result for an entire data file containing many CEADS. To investigate the character of each shock passage and the flow downstream of any given shock, the cross correlation based on only 1 CEADS would be needed. Since meaningful cross correlations cannot be calculated from a single CEADS, the same analysis process as previously described was used but on 10 CEADS. With 10 CEADS adequate definition in the cross correlation can be obtained. Thus the data file was examined exactly as before, but after 10 CEADS had been cross correlated, the result was stored to compare with results at other times in the signal. This process was repeated until the entire data file had been analyzed resulting in hundreds of "10 CEADS" cross correlations.

The 10 CEADS results were examined and were judged as having or not having the separated flow character. Approximately 15% of the plots were judged as not separated on the basis that they did not have the distinct double peak pattern. To assess whether this number was significant relative to signals from continuously separated flow, the flow downstream of *S* was analyzed the same way. Approximately 13% of its 10

CEADS plots were judged as lacking the separated character, which is consistent with the result described above. Thus it is reasonable to conclude that the flow downstream of the shock is separated at all times, and that the instantaneous separation point is essentially at or very close to the separation shock position.

In summary, the intermittent region is also a region of intermittent boundary-layer separation. The well-defined separation line found using surface tracer methods is at or very close to the downstream boundary of the region of intermittent separation. A physical explanation for this result, based on the response of surface tracers to a time-averaged wall shear stress, was suggested earlier in Ref. 13.

Conclusions

A method of detecting flow direction downstream of the unsteady separation shock using fluctuating wall-pressure signals has been developed and tested in a Mach 5 shock-wave, turbulent boundary-layer interaction induced by a circular cylinder. In this method, flow direction is deduced from cross correlations of that part of the pressure signal downstream of the moving shock wave. The results show the following:

1) For both cylinder flows the cross correlations have a maximum at negative time delay indicating that backflow exists immediately downstream of the shock. This result holds at all stations in the intermittent region.

2) The instantaneous separation point is at or close to the instantaneous shock foot in the intermittent region, and hence the separation point itself undergoes a large-scale, streamwise motion. It appears that the well-defined separation line from the kerosene lampblack pattern is at or close to the downstream boundary of a region of intermittent separation.

Appendix

Conditional sampling/analysis algorithms are a relatively new type of technique being used in interactive flows. When data are converted into signals such as boxcars (0 or 1) for shock-motion analysis for instance, or split into different segments based on given criteria, the sensitivity of the method to the decision criteria must be investigated. This was recently discussed by Dolling and Brusniak[6] regarding boxcar analysis. To confirm the validity of the conditional-analysis, cross-correlation code, a threshold sensitivity analysis was performed.

Figure 9 shows the conditional-analysis, cross-correlation results for different thresholds for the same set of data. Two cases are shown for clarity. Although the magnitudes of the coefficients have changed, the maxima of R_{pp} remain at the same time delays (τ). This was also observed for several other threshold combinations. Thus, although the values of $R_{pp\max}$ vary, the corresponding values of τ are insensitive to changes in threshold values.

A similar result is obtained when comparing algorithms. Figure 9 also shows results for both algorithms. Each case had the same thresholds. The top finding algorithm had fewer CEADS which met the 32-point data set requirement due to the stricter requirement of starting the data set with the maximum point past the first threshold, PT1. As a result, more fluctuations due to the shock passage were eliminated, and the corresponding correlation values due to flow behind the shock are slightly higher. However, the time delay values for the peaks remain unaffected.

Acknowledgments

This work was sponsored in part by AFOSR Grant 86-0112 (monitored by L. Sakell), ARO Graduate Fellowship DAALO3-6-0045 (monitored by R. Singleton), and the Center for Hypersonics Training and Research at the University of Texas at Austin (supported by NASA, AFOSR, and ONR). These sources of support are gratefully acknowledged.

References

[1]Settles, G. S., "An Experimental Study of Compressible Turbulent Boundary Layer Separation at High Reynolds Numbers," Ph.D. Dissertation, Mechanical and Aerospace Engineering Dept., Princeton Univ., Sept. 1975.

[2]Dolling, D. S., and Murphy, M. T., "Unsteadiness of the Separation Shock Wave Structure in a Supersonic Compression Ramp Flowfield," *AIAA Journal*, Vol. 21, Dec. 1983, pp. 1628–1634.

[3]Dolling, D. S., and Or, C. T., "Unsteadiness of the Shock Wave Structure in Attached and Separated Compression Ramp Flowfields," *Experiments in Fluids*, Vol. 3, 1985, pp. 24–32.

[4]Muck, K. C., Dussauge, J. P., and Bogdonoff, S. M., "Structure of the Wall Pressure Fluctuations in a Shock-Induced Separated Turbulent Flow," AIAA Paper 85-0179, Jan. 1985.

[5]Dolling, D. S., and Narlo, J. C., II, "Driving Mechanism of Unsteady Separation Shock Motion in Hypersonic Interactive Flow," AGARD CP-428, April 1987.

[6]Dolling, D. S., and Brusniak, L., "Separation Shock Motion in Fin, Cylinder, and Compression Ramp-Induced Turbulent Interactions," *AIAA Journal*, Vol. 27, No. 6, 1989, pp. 734–742.

[7]Smith, D. R., and Dolling, D. S., "Unsteady Shock-Induced Turbulent Separation in Mach 5 Cylinder Interactions," *AIAA Journal*, Vol. 27, No. 12, 1989, pp. 1698–1706.

[8]Eaton, J. K., Jeans, A. H., Ashjaee, J., and Johnston, J. P., "A Wall-Flow Direction Probe for Use in Separating and Reattaching Flows," *Journal of Fluids Engineering*, Vol. 101, Sept. 1979, pp. 364–366.

[9]Westphal, R. V., Eaton, J. K., and Johnston, J. P., "A New Probe for Measurement of Velocity and Wall Shear Stress in Unsteady, Reversing Flow," *Journal of Fluids Engineering*, Vol. 103, Sept. 1981, pp. 478–482.

[10]Dolling, D. S., and Bogdonoff, S. M., "Scaling of Interactions of Cylinders with Supersonic Turbulent Boundary Layers," *AIAA Journal*, Vol. 19, No. 5, May 1981, pp. 655–657.

[11]Raman, K. R., "A Study of Surface Pressure Fluctuations in Hypersonic Turbulent Boundary Layers," NASA CR-2386, Feb. 1974.

[12]Tran, T. T., "An Experimental Investigation of Unsteadiness in Swept Shock Wave/Turbulent Boundary Layer Interactions," Ph.D. Dissertation, Mechanical and Aerospace Engineering Dept., Princeton Univ., Oct. 1986.

[13]Gramann, R. A., and Dolling, D. S., "Interpretation of Separation Lines from Surface Tracers in Shock Induced Turbulent Flow," *AIAA Journal*, Vol. 25, No. 12, 1987, pp. 1545–1546.